RESEARCH PAPER

Nucleus 4:1, 61–73; January/February 2013; © 2013 Landes Bioscience

Soft substrates normalize nuclear morphology and prevent nuclear rupture in fibroblasts from a laminopathy patient with compound heterozygous *LMNA* mutations

Chiara Tamiello,[1,*] Miriam A.F. Kamps,[2,3] Arthur van den Wijngaard,[4] Valerie L.R.M. Verstraeten,[3] Frank P.T. Baaijens,[1] Jos L.V. Broers[2] and Carlijn C.V. Bouten[1]

[1]Department of Biomedical Engineering; Eindhoven University of Technology; Eindhoven, The Netherlands; [2]Department of Molecular Cell Biology; Cardiovascular Research Institute Maastricht; Maastricht University Medical Centre; Maastricht, The Netherlands; [3]Department of Dermatology; Maastricht University Medical Centre; GROW-School for Oncology and Developmental Biology; Maastricht, The Netherlands; [4]Department of Clinical Genetics; Cardiovascular Research Institute Maastricht; Maastricht University Medical Centre; Maastricht, The Netherlands

Keywords: lamina, laminopathies, substrate stiffness, nuclear shape alteration, nuclear rupture

Laminopathies, mainly caused by mutations in the *LMNA* gene, are a group of inherited diseases with a highly variable penetrance; i.e., the disease spectrum in persons with identical *LMNA* mutations range from symptom-free conditions to severe cardiomyopathy and progeria, leading to early death. *LMNA* mutations cause nuclear abnormalities and cellular fragility in response to cellular mechanical stress, but the genotype/phenotype correlations in these diseases remain unclear. Consequently, tools such as mutation analysis are not adequate for predicting the course of the disease.

Here, we employ growth substrate stiffness to probe nuclear fragility in cultured dermal fibroblasts from a laminopathy patient with compound progeroid syndrome. We show that culturing of these cells on substrates with stiffness higher than 10 kPa results in malformations and even rupture of the nuclei, while culture on a soft substrate (3 kPa) protects the nuclei from morphological alterations and ruptures. No malformations were seen in healthy control cells at any substrate stiffness. In addition, analysis of the actin cytoskeleton organization in this laminopathy cells demonstrates that the onset of nuclear abnormalities correlates to an increase in cytoskeletal tension.

Together, these data indicate that culturing of these *LMNA* mutated cells on substrates with a range of different stiffnesses can be used to probe the degree of nuclear fragility. This assay may be useful in predicting patient-specific phenotypic development and in investigations on the underlying mechanisms of nuclear and cellular fragility in laminopathies.

Introduction

The structural continuity between the intracellular (nucleus and cytoskeleton) and the extracellular environment of adherent cells is crucial for cell fate.[1,2] The coupling between nucleus and cytoskeleton via proteins embedded in the nuclear envelope and the connection between cytoskeletal filaments and the extracellular matrix (ECM) via focal adhesions, together are part of the mechanotransduction mechanism, i.e., the process of converting physical forces into biochemical signals and integrating these signals into cellular responses.[3-5]

Some of the structural connections between the nucleus and the cytoskeleton are altered by mutations in the *LMNA* gene, which encodes for lamina-type proteins, i.e., lamin A, lamin C and lamin AΔ10. Lamins are located just underneath the inner nuclear membrane of most differentiated somatic cells and form the nuclear lamina, a fibrillar network part of the nuclear envelope which plays a crucial role in the maintenance of nuclear shape and gives structural support to the nucleus.[6,7] Consequent to disturbances in the structural connections with the cytoskeleton and in the nuclear lamina assembly, *LMNA* mutations lead to decreased cellular stiffness and increased mechanical weakness leading to increased sensitivity to mechanical stress.[8,9] Abnormal nuclear morphology, compromised nuclear integrity and tendency to spontaneous nuclear disruption, even in the absence of external forces, are also reported for these cells.[8-16]

The family of genetic diseases associated with mutations in the *LMNA* gene is called laminopathies. Laminopathies are associated with a diverse array of tissue-specific degenerative disorders as well as syndromes with overlapping features. The most important pathologies included are: different types of striated muscle diseases, such as Limb-girdle muscular dystrophy, Emery-Dreifuss muscular dystrophy and dilated cardiomyopathy; abnormalities in adipose tissue development, including familial partial lipodystrophy, type II (Dunningan syndrome) and type II diabetes; peripheral nerve diseases such as Charcot Marie-Tooth

*Correspondence to: Chiara Tamiello; Email: c.tamiello@tue.nl
Submitted: 09/19/12; Revised: 12/19/12; Accepted: 12/21/12
http://dx.doi.org/10.4161/nucl.23388

disease and systemic failure diseases such as Hutchinson Gilford progeria syndrome (premature aging). Most of the symptoms develop in the postnatal phase and may lead to early death.[17] The molecular mechanisms giving rise to tissue-specific laminopathies are still largely unknown. The complexity of these diseases is further exemplified by the fact that identical genetic mutations can give rise either to a severe disease phenotype in one patient or no clinical symptoms at all in another person. These observations indicate that mutation analysis alone is not conclusive for diagnosis or prognosis of laminopathy development and consequent functional losses.

Here we propose to use cell culture on substrates with different stiffness to probe laminopathy cells from a progeroid syndrome patient with compound heterozygous mutations in the *LMNA* gene, consisting of p.T528M in combination with p.M540T.[18] We hypothesize that soft substrates can protect nuclei of these laminopathy cells from morphological disturbances and structural weakness, as in this case lower forces are propagated to the weakened nucleus. We examined dermal fibroblasts from the laminopathy patient and healthy control dermal fibroblasts seeded on collagen-I coated polyacrylamide gels (PA gels) with stiffness varying over a physiologic range (3–80 kPa) and glass substrates as control. After 48 h from seeding, we analyzed nuclear shape and rupture, as well as actin cytoskeleton organization, which is the main determinant of cell shape, structure and cellular stiffness.[19-21] Our results show that that only on soft substrates (3 kPa) the laminopathy cells tested respond similar to healthy control cells. Interestingly, we were able to probe the intracellular response of these cells by varying the stiffness of the extracellular environment. This suggests that modulation of substrate stiffness is an attractive tool to investigate mechanical functioning and fragility of genetically affected cells of individual patients as a phenotypic marker of the disease stage.

Results

We investigated the intracellular effect of increasing substrate stiffness on diseased dermal fibroblasts, isolated from a patient suffering from a progeroid syndrome due to compound heterozygous missense mutations (p.T528M and p.M540T) in the *LMNA* gene (*LMNA*mut) and we compared these findings with control human fibroblast cell line (NHDFα). For this purpose both cell types were seeded on collagen I coated polyacrylamide (PA) gels with stiffnesses ranging from 3 kPa to 80 kPa, as well as on collagen I coated glass substrates. Both cell types adhered and elongated when plated on the surface of the collagen I coated PA gels and glass substrates, except for the 3 kPa where fewer cells adhered and reduced cell spreading after attachment was observed after 48 h from seeding (**Fig. 1A**). Fluorescent staining (phalloidin-TRITC) of the actin cytoskeleton at 48 h after seeding suggested that both cell types could equally sense the stiffness of the substrates as their actin cytoskeleton became more stretched and organized in bundles for substrates stiffer than 3 kPa (**Fig. 1B**). Quantitative measurement of cell area and aspect ratio confirmed that soft substrates (3 kPa) with E = 3 kPa elicit significant lower cell spreading and elongation in both cell types (**Fig. 1C and D**). However, no significant differences were observed on the 10, 20, 80 kPa PA gels and glass.

Nuclear shape of *LMNA*mut is abnormal on stiff substrates but preserved on soft substrates. Morphologically visible nuclear abnormalities are common in laminopathy cells.[22] These abnormalities, seen as nuclear blebs, herniations and so-called honeycomb structures after immunostaining, seem to indicate the presence of weak spots at the nuclear membrane and/or nuclear interior. Here, we tested whether the extracellular substrate stiffness affects the frequency of these nuclear abnormalities in the *LMNA*mut cells. From the images of DAPI and lamin B1 immunolabeled nuclei, it became obvious that few abnormally shaped nuclei were seen in cells seeded at low stiffness after 48 h from seeding (between 3 and 4% of all nuclei) (**Fig. S1**). Representative images of normal and abnormally shaped nuclei are shown in **Figure 2A**. Further quantitative analysis of 600 nuclei per cell genotype showed that on soft substrates (3 kPa) both *LMNA*mut and NHDFα nuclei overall have a normal appearance (2.9 ± 0.4% NHDFα, 3.7 ± 0.4% *LMNA*mut, **Fig. 2B**). However, while in the NHDFα control fibroblasts abnormally shaped nuclei were detected in about 3.0 ± 0.7% of the cells regardless of the substrate stiffness, a significant increase of abnormally shaped *LMNA*mut nuclei was observed on 10, 20, 80 kPa PA gels and glass substrates (respectively 8.2 ± 0.7%, 26.9 ± 5.0%, 44.7 ± 1.7%, 22.5 ± 2.4%) (**Fig. 2B and C**). The fraction of misshapen nuclei in *LMNA*mut cells increased significantly on the 80 kPa gel (up to 44.7 ± 1.7% compared with 26.9 ± 5.0% on 20 kPa). A reason for this significant increase could be the higher cell density observed on the 80 kPa gels seeded with LMNAmut cells. As in a side experiment we observed increased nuclear aberrations with increased cell density, we therefore hypothesize that cell-cell contact played a role in the formation of nuclear abnormalities (**Fig. S2**). On the glass substrate results were similar to those on the 20 kPa PA gels (22.5 ± 2.4%). The findings on glass are in agreement with earlier studies, showing that 36% of all cells from this *LMNA*mut patient cultured on glass substrates had irregularly shaped nuclei with blebs, honeycomb figures, large and poorly defined protrusions.[18]

***LMNA*mut cells show a defective actin cytoskeleton on stiff substrates but not on soft substrates.** In order to provide insight into the role of the actin cytoskeleton on the onset of nuclear abnormalities (protective mechanism of a soft environment on nuclear integrity), we investigated actin fiber organization using phalloidin-TRITC labeling. The actin cytoskeleton is known indeed to respond to substrate stiffness and affect cell shape and migration. Confocal microscopy of the phalloidin stained cells plated on 3 kPa PA gels showed a rounded morphology for both cell genotypes, with little polymerized actin formation that barely formed bundling of tensed fibers. In the perinuclear region there seemed to be no actin fibers, while we observed fibers running on top of the nucleus (actin cap) (**Fig. 3A**). At 10 kPa and higher stiffnesses, cells demonstrated the typical well-spread and flattened morphology with development of bundles of tense stress fibers (**Figs. 1A and 3B**). According to Khatau

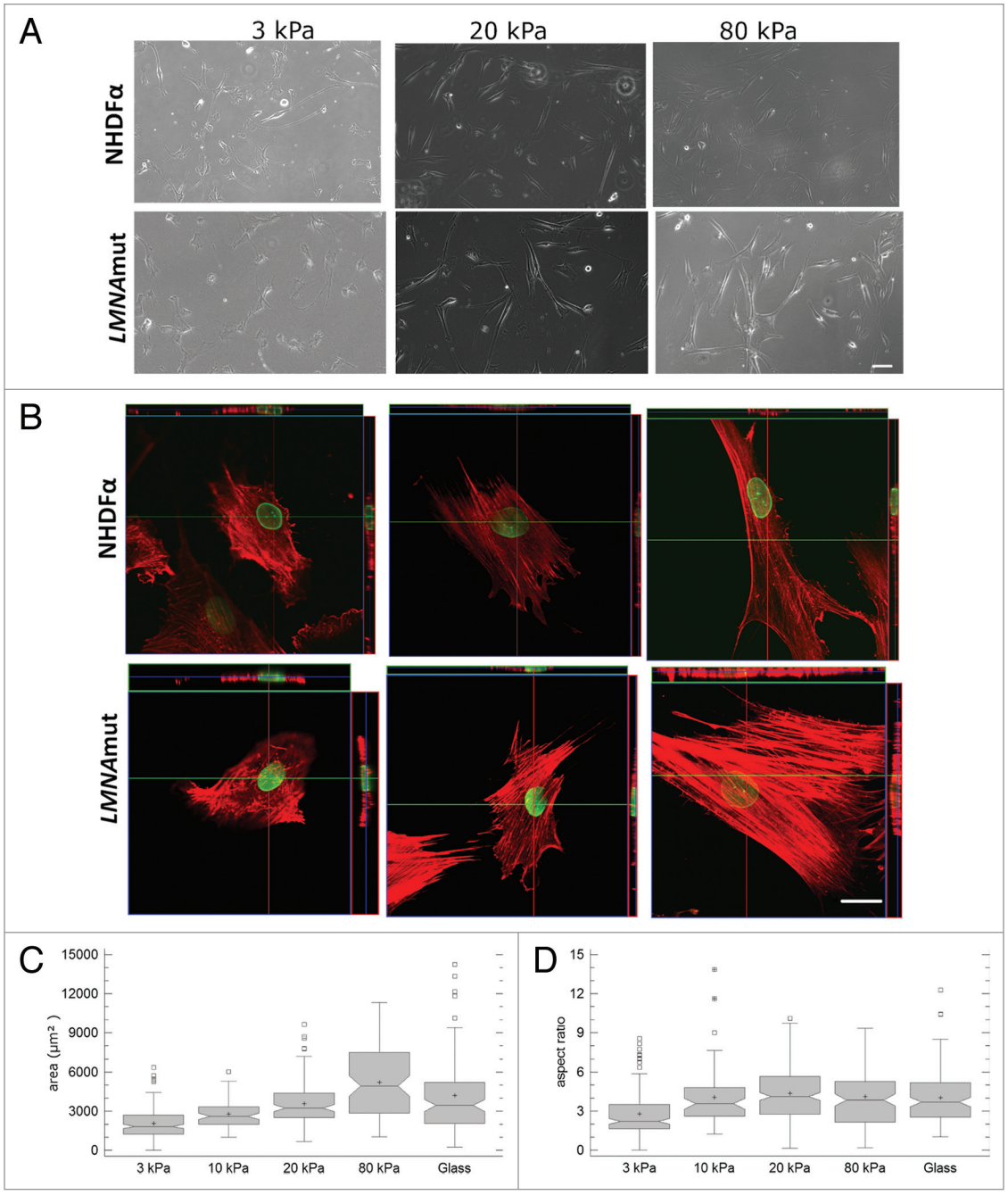

Figure 1. Effect of substrate stiffness on cell morphology and actin cytoskeleton organization. (**A**) Representative bright field images of NHDFα and *LMNA*mut cells seeded on polyacrylamide gels with stiffness ranging from 3 kPa to 80 kPa taken 48 h after seeding. Fewer and less spread cells were present on 3 kPa polyacrylamide gels than on stiffer substrates for both cell types. Scale bar: 100 μm. (**B**) Actin organization in NHDFα and *LMNA*mut (phalloidin-TRITC, red) showed increased organization and tension on substrates stiffer than 3 kPa. Green color is given by lamin B1 staining. Scale bar: 20 μm. (**C and D**) Cell area and aspect ratio presented as box-and-whisker plots. The measurements of NHDFα and *LMNA*mut did not show significant difference, thus the values were considered as a group.

et al.,[23] *LMNA* mutant cells can lack the characteristic actin cap running above the nucleus. After analysis of confocal z-stacks of both cell genotypes in our study, we could not confirm a difference in actin cap presence. However, we did detect aberrations in actin cytoskeleton organization in about 5% of the *LMNA*mut cells plated on 10, 20, 80 kPa and glass, at 48 h after seeding but not on the 3 kPa. These aberrations included detachment of actin stress fibers in the perinuclear region with formation of a speckled pattern of actin which suggests actin depolymerisation in these areas (**Fig. 3C–E**). Similar observations were already reported for cells cultured on glass coverslips.[7,17,24,25]

Disruptions of the actin-cytoskeleton and trypsinization partially normalize nuclear abnormalities in *LMNA*mut cells. To further prove the correlation between actin cytoskeletal

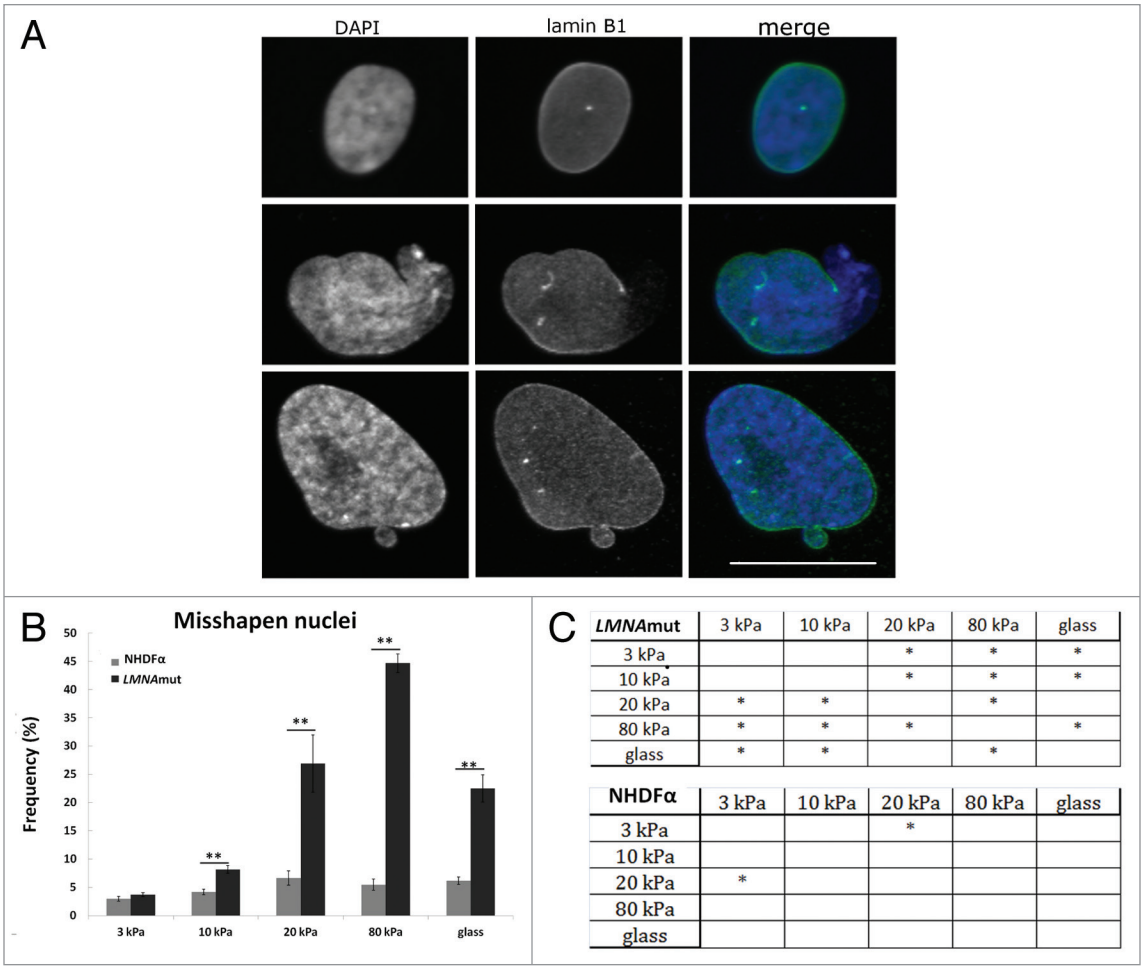

C

*LMNA*mut	3 kPa	10 kPa	20 kPa	80 kPa	glass
3 kPa			*	*	*
10 kPa			*	*	*
20 kPa	*	*		*	
80 kPa	*	*	*		*
glass	*	*		*	

NHDFα	3 kPa	10 kPa	20 kPa	80 kPa	glass
3 kPa			*		
10 kPa					
20 kPa	*				
80 kPa					
glass					

Figure 2. Nuclear morphological abnormality regulation by substrate stiffness. (**A**) Immunofluorescent labeling of cell nuclei with DAPI (blue), lamin B1 (green) and overlay of the two in the most right panels allowed to distinguish between normally (upper row) and abnormally shaped nuclei (second and third row). In particular, the nucleus in the second row shows a protrusion and in the third row a bleb can be observed. Scale bars: 10 μm. (**B**) Frequency of abnormally shaped nuclei on increasing PA gel stiffness for *LMNA*mut and control NHDFα. Values represent means from at least 300 cells from two experiments. Bars represent SEM * $p < 0.05$, ** $p < 0.01$ vs NHDFα on the same substrate stiffness (**C**) Statistical analyses of differences in frequency of misshapen nuclei for *LMNA*mut and NHDFα on the different substrate stiffness's. *, $p < 0.05$; no star, $p > 0.05$.

tension and the onset of nuclear abnormalities, *LMNA*mut cells grown on collagen I coated glass bottom culture dishes were incubated for different period of times with cytochalasin D (cytoD), which inhibits actin dynamics and, consequently, causes disruption of the actin-cytoskeleton (**Fig.** 4). Next, the drug was removed and *LMNA*mut cells were allowed to recover in normal growth medium for 1 h to overnight. Confocal microscopy on phalloidin-TRITC and DAPI stained *LMNA*mut cells showed that the short treatment (30 min) followed by 1 h recovery (short treatment + short recovery) disrupted the actin-cytoskeleton only mildly compared with untreated control *LMNA*mut (**Fig. 4A and B**). Yet, there was no difference between the frequency of misshapen nuclei in this group and in the untreated control *LMNA*mut (18.4 ± 2.1% vs 22.3 ± 4.0%, **Fig. 4E**). There was presumably not enough time for the nucleus to respond to the decrease in cytoskeletal tension or the degree of disruption did not allow any response. In contrast, a three hour treatment followed by an hour recovery (long treatment + short recovery) leads to serious disruption of the actin cytoskeleton and significantly less misshapen nuclei (11.8 ± 0.8%, **Fig. 4C**). Upon three hours cytoD treatment followed by overnight recovery (long treatment + long recovery), the actin cytoskeleton completely recovered from the treatment and tensed stress fibers were visible (**Fig. 4D**). The frequency of misshapen nuclei (19.1 ± 1.6%) was found to be comparable to that of untreated *LMNA*mut cells. Moreover we analyzed the changes in nuclear morphology due to cellular detachment of *LMNA*mut cells by trypsin, followed by re-adhesion to a glass substrate (**Fig. 5**). At 30 and 60 min after seeding, nuclear folding due to trypsin treatment did not yet allow a reliable analysis of nuclear shape. At this stage of attachment the actin cytoskeleton was largely disorganized, seen as absence of tense stress fibers in these cells. Starting from 2 till 8 h after seeding the frequency of misshapen nuclei was significantly lower than that at 72 h (11.0 ± 2.0%, 13.3 ± 3.8%, 14.6 ± 2.3%, 15.6 ± 2.2%, 28.3 ± 3.5% respectively at 2, 4, 8, 24 and 72 h). At these time points actin reorganization did take place in the lower

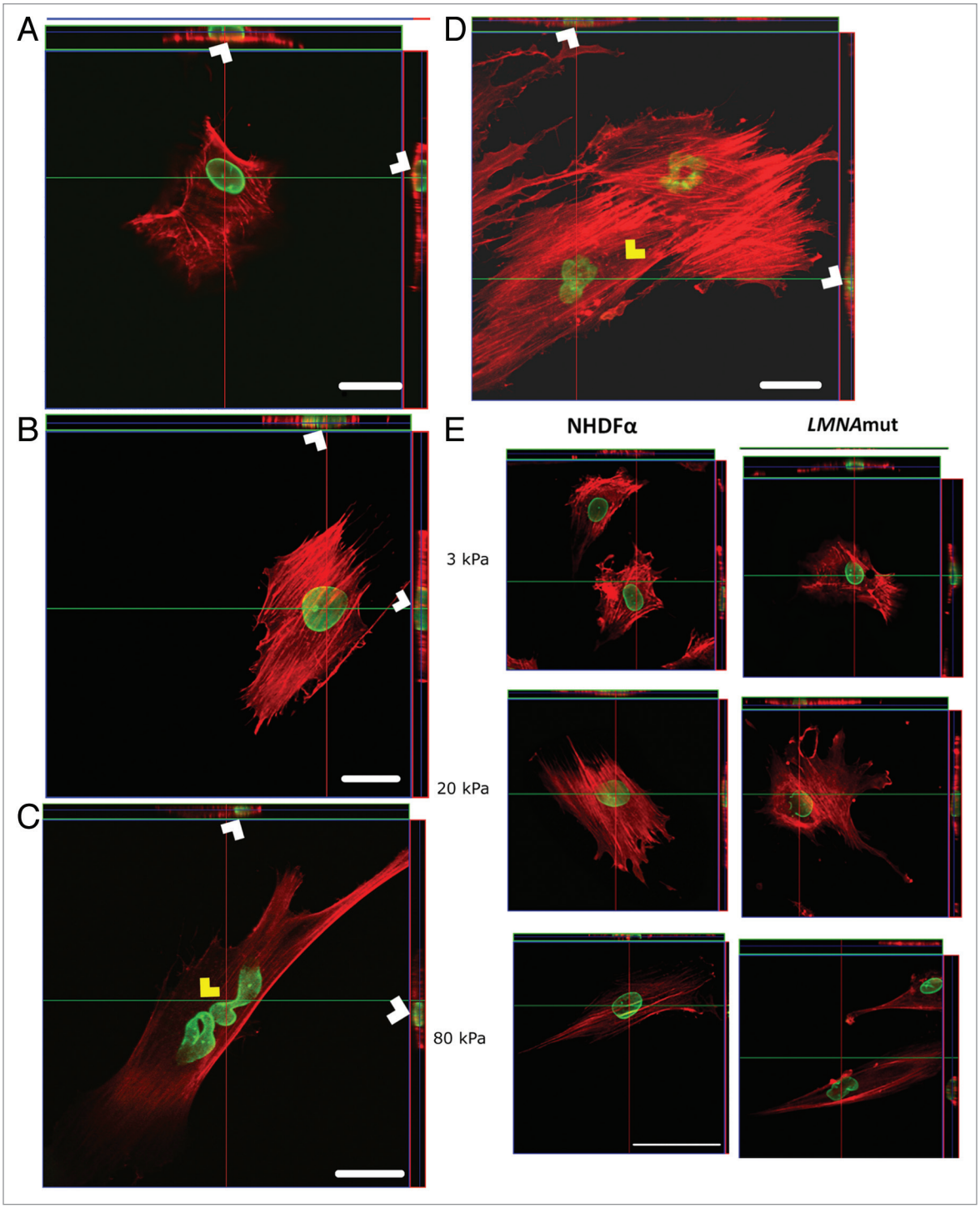

Figure 3. Influence of substrate stiffness on cytoskeletal actin organization and aberrations. Confocal z-series taken from half height of the whole cell and relative orthogonal cross sections of NHDFα and *LMNA*mut immunocytochemical stained for F-actin in red (phalloidin-TRITC) and Lamin B1 in green at 48 h after seeding. (**A**) Representative fibroblast seeded on 3 kPa PA gels. It shows short and not tensed actin fibers, which are missing in the perinuclear region. An actin cap is running above the nucleus (white arrowhead). No differences could be noticed between *LMNA*mut and NHDFα. Thus no aberrations could be detected in the actin cytoskeleton of cells plated on soft substrates. (**B**) Control NHDFα on PA gel stiffer than 3 kPa, precisely on the 20 kPa PA gel. Actin stress fibers are tensed and well-structured also in the perinuclear region. The actin cap made of thick stress fibers run above the nucleus the (white arrowhead) nucleus. (**C and D**) Representative aberrations found in *LMNA*mut seeded on 20 (**C**) and 80 kPa (**D**) PA gels. Cells have a misshapen nucleus. Yellow arrowhead indicates the lack of actin fibers in the perinuclear region (**D and E**) and a speckled distribution of actin (**E**). The actin cap is running above the nucleus (white arrowhead). Scale bars: 20 μm. (**E**) Representative images of cells on three substrate stiffnesses. NHDFα (left panel) and *LMNA*mut (right panel) on 3 kPa (F), 20 kPa (G) and 80 kPa (H) PA gels. Scale bar: 50 μm.

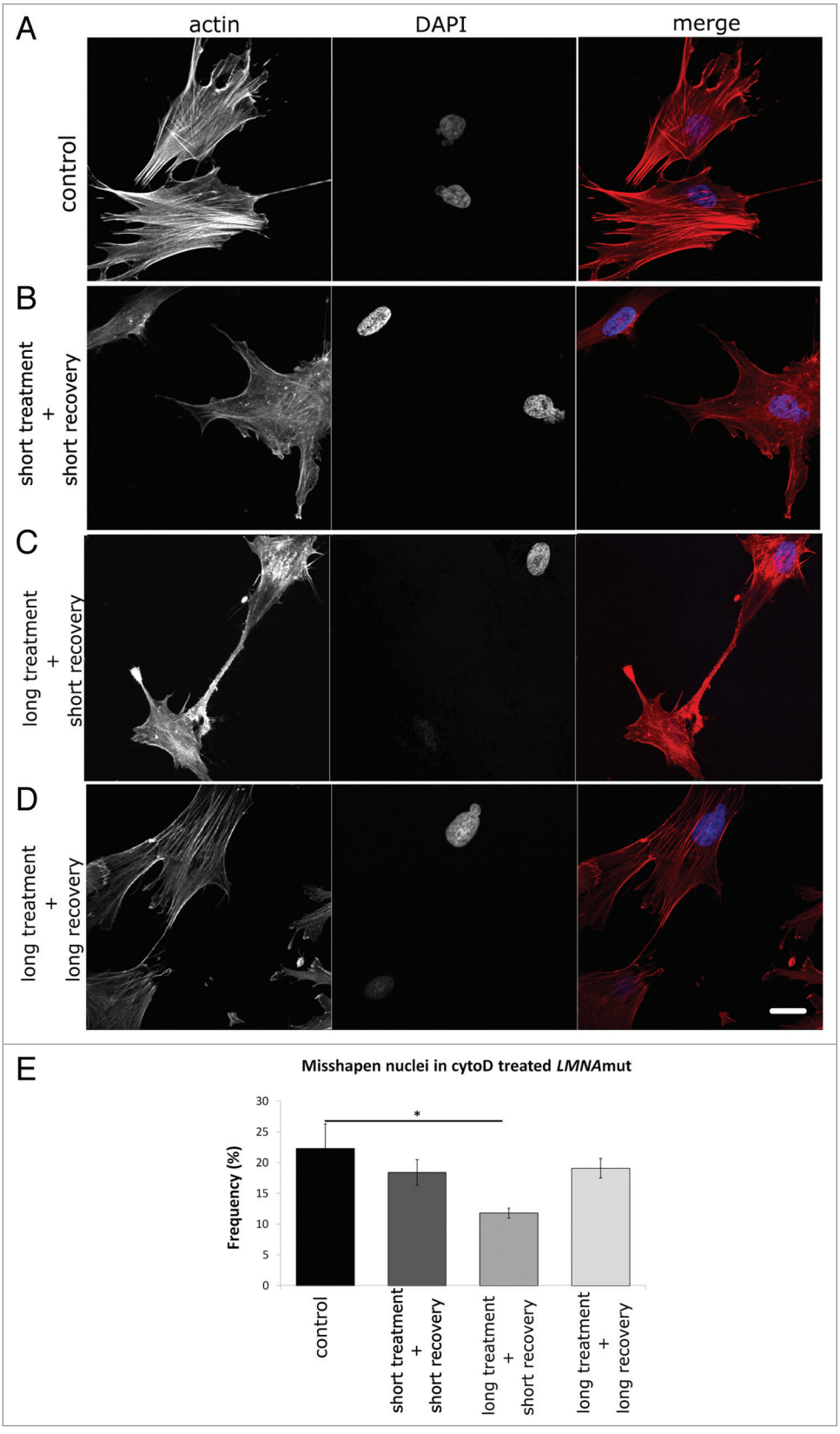

Figure 4. Effects of transient cytoD treatment on *LMNA*mut nuclei. Representative confocal sections of *LMNA*mut seeded on collagen I coated glass substrates incubated with cytoD 1μM and recovered in normal growth medium. After fixation, cells were stained with DAPI (blue) to check for nuclear abnormalities and phalloidin-TRITC (red) to check for actin organization. (**A**) Untreated control *LMNA*mut. (**B**) Short treatment + short recovery: *LMNA*mut treated for 30 min with cytoD and recovered for 1 h. (**C**) Long treatment + short recovery: *LMNA*mut treated for 3 h with cytoD and recovered for 1 h. (**D**) Long treatment + long recovery *LMNA*mut treated for 3 h with cytoD and recovered overnight. Scale bar: 20 μm. (**E**) Frequency of misshapen nuclei in *LMNA*mut upon treatment with cytoD. At least 600 cells were assessed per each group.*, $p < 0.05$; no star, $p > 0.05$.

regions of the cell, making contact with the glass substrate, but stress fibers were absent at close distance to the nucleus. While after 24 h of attachment the actin organization was mainly restored, showing actin fibers in close contact with the nucleus, it took even longer (up to 72 h) until cells were fully stretched, and showing the regular percentage of abnormal nuclei (**Fig. 5A and B**).

Strikingly, not only the number of cells with blebs, but also bleb size itself increased considerably with time, ranging from 1–25 μm^2 after 2 h (average 5.24 μm^2, n = 12) to 3–62 μm^2 (average 24.4 μm^2, n = 10, **Fig. 5C**). This shows that nuclear morphology becomes partially normalized after trypsinization, which hydrolyzes the protein-protein bonds that attach cells to the extracellular matrix and consequently induces cell rounding along with reduction of cytoskeletal tension.

All together, these results suggest a direct correlation between the level of actin-cytoskeleton tension and the prominence of nuclear abnormalities.

Cellular compartmentalization in *LMNA*mut cells is not compromised on soft substrates. Given the increased presence of abnormally shaped nuclei in LMNAmut cells cultured on substrates stiffer than 3 kPa, we tested whether this was correlated with a loss of cellular compartmentalization. We chose promyeolocytic leukemia nuclear bodies (PML-NBs) as marker, as these assemblies of PML proteins are normally confined to

the nuclear interior of non-proliferating cells (**Fig. 6A**).[26] Earlier studies by De Vos et al. and Houben et al. showed that frequent loss of PML-NBs from the nucleus to the cytoplasm can be found in laminopathy cells.[14,27,28] In the current experiment, approximately 600 cells for each genotype, on each substrate, were screened manually for PML-NBs localization using fluorescent microscopy. We observed cytoplasmic PML-NBs (cytPML-NBs) in cases of abnormally shaped nuclei as well as for intact nuclei (**Fig. 6B and C**). Therefore it is not possible to directly correlate abnormalities in the nuclear shape to the loss of cellular compartmentalization. Similarly to previous findings,[14] 4.4 ± 1.1% NHDFα control cells demonstrated cytPML-NBs, regardless of the substrate stiffness. On the 3 kPa substrate, *LMNA*mut and NHDFα control cells showed no significant differences in the frequency of cells with cytPML-NBs (3.1 ± 0.5% *LMNA*mut and 2.0 ± 0.2% NHDFα). However, we did observe a gradual increase of *LMNA*mut cells with cytPML-NBs with increasing stiffness of the substrates between 3 and 20 kPa (from 3.1 ± 0.5% to 12.8 ± 1.2%), indicating increased frequency of cytPML-NBs in *LMNA*mut cells.

Nuclear ruptures in *LMNA*mut cells increase with substrate stiffness, but are prevented on soft substrates. A recent study by De Vos et al.[16] showed the occurrence of spontaneous nuclear ruptures in cells from laminopathy patients cultured on glass substrates. These ruptures never occurred in wild type cells (NHDFα) under the same culturing conditions. Based on these results and triggered by the finding of variable cytPML-NBs on different substrate stiffness, we hypothesized that mechanical cues provided by the extracellular environment might affect the frequency of nuclear rupture events. For this purpose we monitored living cells (about 20) for two hours at one or two minute intervals under a fluorescent microscope on 3, 10, 20, 80 kPa PA gels and glass substrate after 24–36 h from transfection with EYFP-nuclear localization signal (EYFP-NLS), which helped to check for nuclear integrity. Correct expression of EYFP-NLS was revealed by a constant intense intranuclear fluorescent signal. In NHDFα cells, as well as in *LMNA*mut cells on 3 kPa substrates we could not detect a nuclear rupture event in any cell examined. In contrast, for the stiffer substrates an increased frequency of nuclear rupture was detected in the *LMNA*mut cells, increasing from 20% (4/20) of *LMNA*mut with nuclear rupture on the 10 kPa substrate to 34.5% (10/29) on 80 kPa. The ruptures were visible as a sudden transient efflux of EYFP-NLS from the nucleus to the cytoplasm (**Fig. 7 and Vid. S1**). This phenomenon, which lasts about 20 min and can occur repetitively in the same cell, was followed by restoration of EYFP-NLS signal in the nucleus and was not lethal for the cells. All together, these results confirm that soft substrates do not compromise the nuclear integrity of *LMNA*mut cells, while stiff environments do.

Discussion

In this study we showed that, on soft substrates with stiffness of 3 kPa, abnormal nuclear morphology and nuclear ruptures in dermal fibroblasts from a laminopathy patient with compound heterozygosity for mutations in LMNA can be normalized. Normalization of nuclear shape at low substrate stiffness, i.e., in presence of low cytoskeletal tension, indicates that nuclear abnormalities correlate to the mechanical properties of the ECM, such as the collagen I-coated PA gels used in here. For the purpose of this study and in view of a future clinical application, we chose to investigate dermal fibroblasts because it is and easily accessible cell source to probe and investigate.[29]

A crucial finding is that the nuclei of *LMNA*mut cells used in this study do not develop an abnormal morphology when they are cultured on soft gels (3 kPa), while on stiffer substrates nuclei appear to have a misshapen shape (**Fig. 2**) as reported also by Verstraeten et al.[18] Abnormal nuclear phenotypes are normally found in cells with *LMNA* mutations,[10,11,18,30] but the relevance of morphological abnormalities in the pathogenesis of laminopathies is not unravelled. Nuclear abnormalities are indeed not present in all diseased cells and there is no direct association between nuclear abnormalities and disease phenotype or severity.[31] However, previous studies have been performed only on glass or stiff silicon substrates and did not consider the mechanotransduction feedback-loop, which influences the cellular response based on the ECM mechanical cues. Still, in order to establish correlations between genotype and phenotype repeated measures using cells from different patients or families of patients are needed, as the phenotypic variability in this family of diseases may lead to different responses of the nucleus to developing intracellular tension.

One reason for increased nuclear abnormalities, nuclear ruptures and loss of cellular compartmentalization might be that, on soft substrates, the nuclear membrane is exposed to reduced cytoskeletal forces, transduced from the ECM. This can be inferred by our results on the actin cytoskeleton organization and from the partial normalization of the nuclar abnormalities upon disruption of the actin cytoskeleton by cytoD and after cell trypsinization. When actin is not assembled into tensed stress fibers, it is likely that the force exerted on the nucleus is not enough to tear apart the nuclear membrane or to compress the nucleus, causing nuclear rupture at weak spots.

Furthermore, disorganization of the actin cytoskeleton in the perinuclear region of *LMNA*mut, was observed particularly on stiffer substrates and gave indication for an abnormal distribution of forces exerted to the nucleus, enhancing nuclear morphology disturbance. In contrast to Kathau et al.,[23] we observed in the *LMNA*mut cells the presence of the nuclear shaping actin cap. Therefore, to explain these findings, we propose that a pulling mechanism in addition to a compressive pushing mechanism might play a role in altering nuclear morphology. We suspect that, on stiff substrates, the actin cap presses tightly against the nucleus and, in addition, organization of the stress fibers around the nucleus is abnormal, enhancing the probability of disturbance and rupture in the morphology of the genetically disorganized and weakened nucleus (**Fig. 8**). This physical model can explain the observations on the different substrate stiffnesses. However the significant increase of misshapen nuclei on the 80 kPa PA gel is, in our opinion, due to an increase of cell-cell contact and increase in cell area and

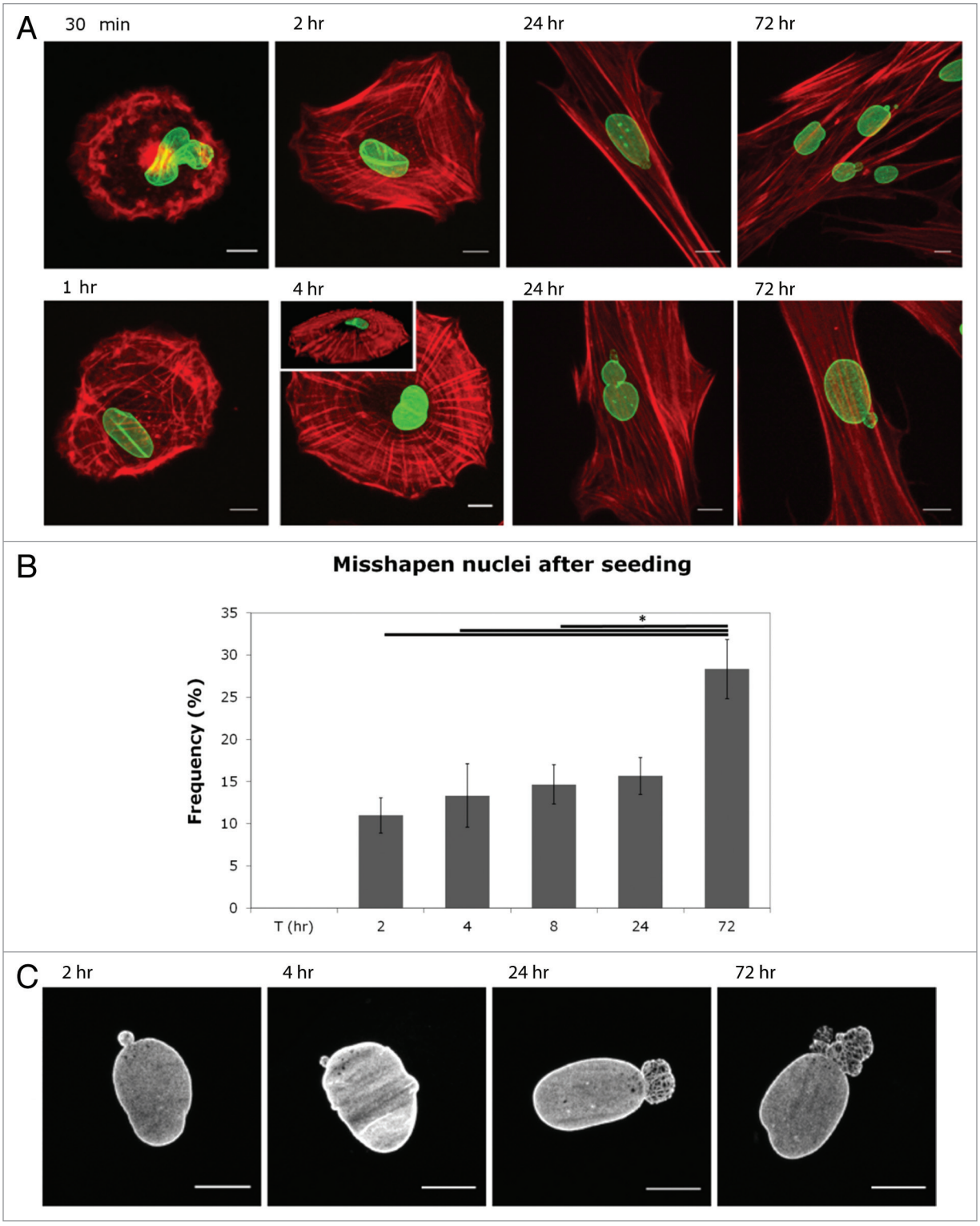

Figure 5. Alterations in nuclear shape and actin organization upon attachment of cells after trypsin treatment. (**A**) Representative confocal sections of *LMNA*mut seeded on collagen I coated glass substrates at 30 min, 1, 2, 4, 24 and 72 h after seeding. Cells were immunocytochemical stained for F-actin in red (phalloidin-TR) and lamin A/C in green. Inset at 4 h: 3D view (generated by ImageJ 3D-viewer, showing the position of the nucleus (green) at the upper region of the cell, with very few tense actin stress fibers (red) surrounding the nucleus). Scale bar: 10 μm. (**B**) Frequency of misshapen nuclei after seeding. *, $p < 0.05$; no star, $p > 0.05$. (**C**) Changes in nuclear bleb size upon attachment, visualized by immunofluorescence using the Jol2 lamin A/C antibody. Note the increase in size as well as the aberrant shape of the nuclear blebs. Note also that in most blebs a typical honeycomb structure of the lamina staining can be seen. Scale bar: 10 μm.

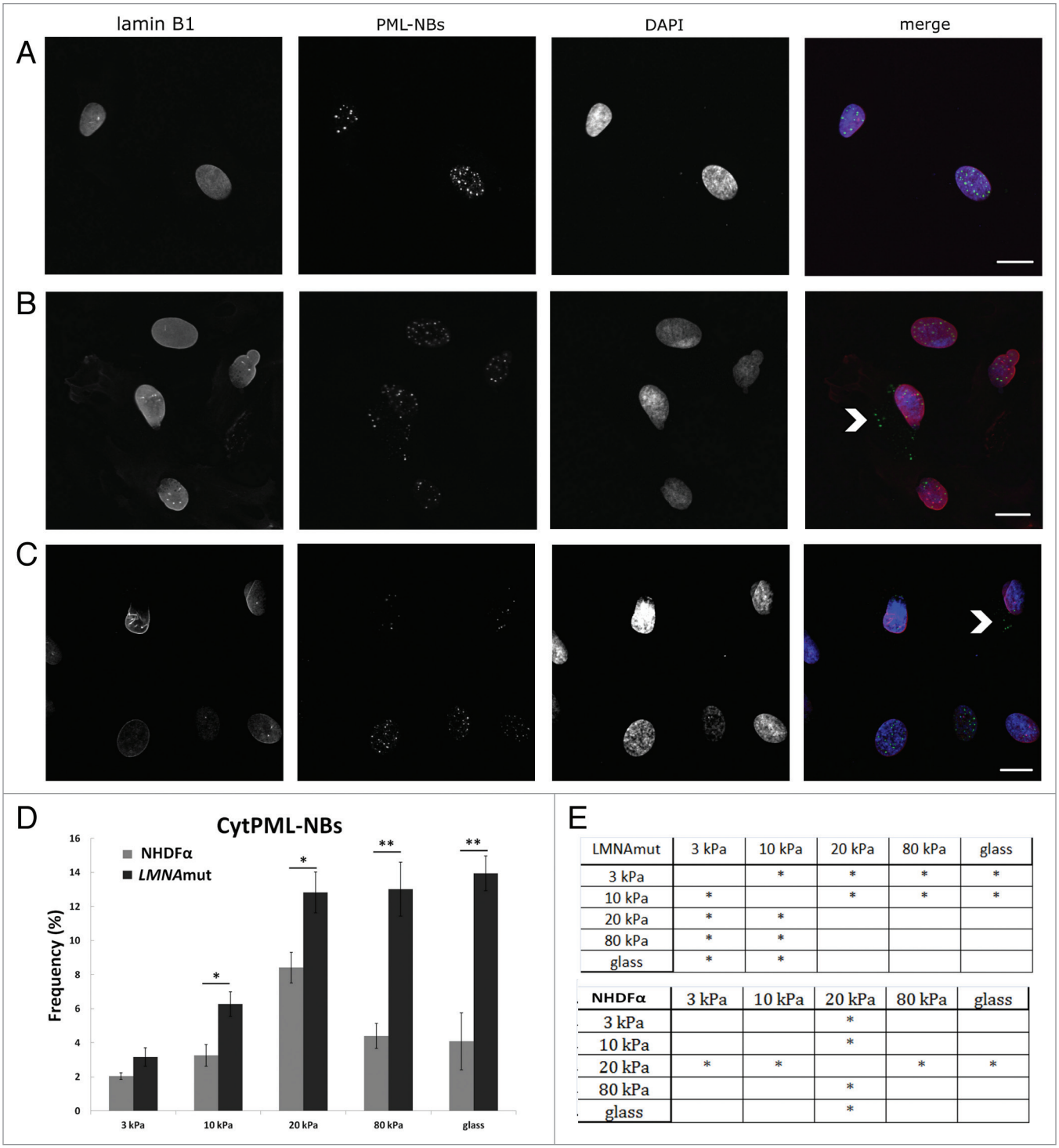

LMNAmut	3 kPa	10 kPa	20 kPa	80 kPa	glass
3 kPa		*	*	*	*
10 kPa	*		*	*	*
20 kPa	*	*			
80 kPa	*	*			
glass	*	*			

NHDFα	3 kPa	10 kPa	20 kPa	80 kPa	glass
3 kPa			*		
10 kPa			*		
20 kPa	*	*		*	*
80 kPa			*		
glass			*		

Figure 6. PML-NBs localization as a marker for cellular compartmentalization. (**A–C**) Confocal sections representative of cell nuclei were immunolabeled with Lamin B1 (red), DAPI (blue) and PML-NBs (green) to investigate the localization of PML-NBs. Nuclei were counterstained with DAPI (blue). The most right panel shows the triple overlay. Scale bars: 10 μm. (**A**) Nuclei showing normal morphology and internal localization of PML-NBs. Cellular compartmentalization is intact. (**B**) Cytoplasmic localization of PML-NBs (cytPML-NBs) around a nucleus showing an abnormal morphology (white arrowhead). Loss of cellular compartmentalization is indicated by the exit of PML-NBs to the cytoplasm. (**C**) CytPML-NBs could be found also in normally shaped nuclei (white arrowhead) indicating that loss of cellular compartmentalization is not directly related to nuclear morphology abnormalities. (**D**) Relative frequency of NHDFα and *LMNA*mut showing cytPML-NBs. Values represent means from at least 600 cells from 2 experiments. Bars represent SEM * $p < 0.05$, ** $p < 0.01$ vs NHDFα on the same substrate stiffness. (**E**) Statistical analyses of differences in frequency of cytPML-NBs for *LMNA*mut and NHDFα on the different substrate stiffness's. *, $p < 0.05$; no star, $p > 0.05$.

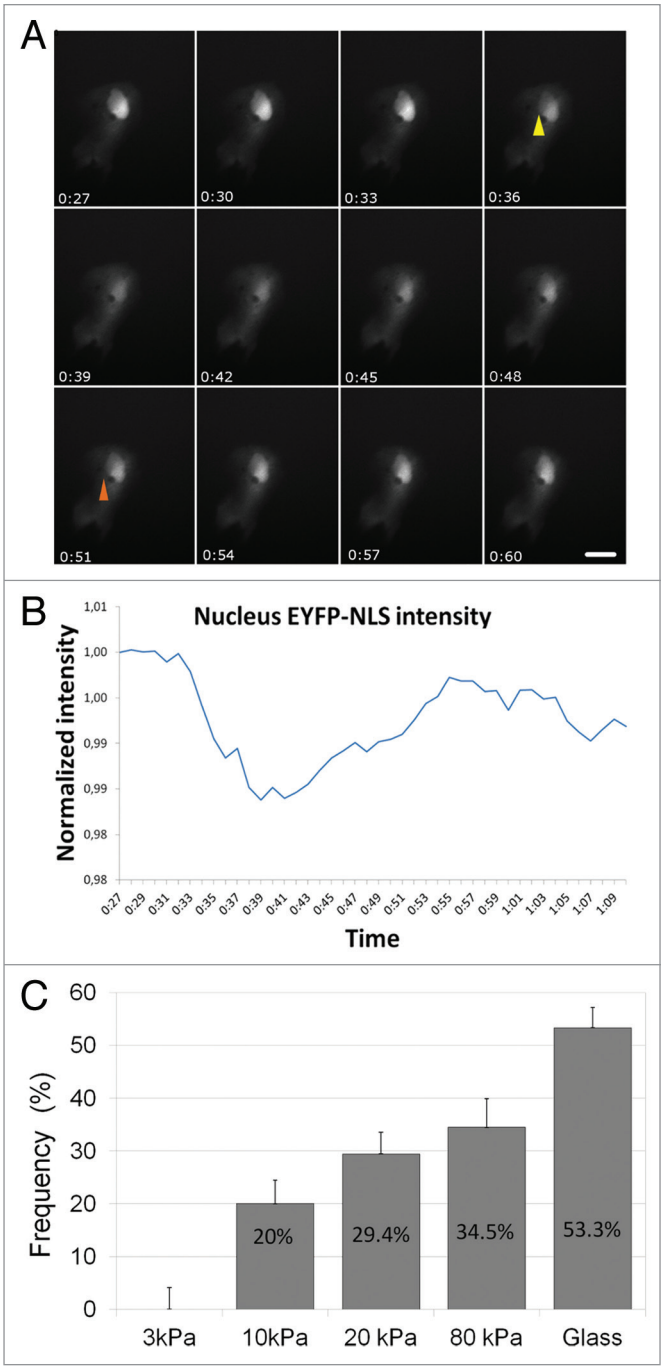

Figure 7. Spontaneous ruptures of the nuclear membrane do not occur on soft substrates. (**A**) Montage of selected images from a time-lapse recording of *LMNA*mut cell cultured on 10 kPa PA gel and transfected with EYFP-NLS, sampled at 1 min intervals for 2 h (**Vid. S1**). Nuclear membrane rupture causes the decrease in intranuclear EYFP signal and increase in cytoplasmic EYFP signal (at 0:36, yellow arrowhead). Subsequently, the nuclear signal is gradually up taken by the nucleus and the rupture appears to be restored (at 0:51, orange arrowhead) (**B**) Evolution in time of EYFP-NLS (mean) intensity in the nucleus of the cell shown in (**A**). (**C**) Frequency of spontaneous nuclear membrane ruptures on the different substrates for *LMNA*mut. Error bars represent the square root of the number of recording.

aspect ratio, which imply increase of cytoskeletal forces exerted on the nucleus. Reasons for the increase in cell area and cell aspect ratio might be found in changes in adhesive properties of the substrates. Hydrogels of increasing stiffnesses lead to increasing anchoring densities and thereby increase in cell spreading,[32] while collagen absorption onto glass substrate could determine an anchoring density similar to that of the 20 kPa PA gel. While these in vitro studies cannot be directly interpolated to the in vivo situation our assay to measure nuclear weakness could well predict the development of a laminopathy phenotype in patients. A common denominator in (nearly) all laminopathies is the loss of specific tissues, seen as muscular dystrophies and/or lipodystrophies. For each of these laminopathies, its value will have to be proven.

Taken together our data suggests that we were able to probe the response of the nucleus from the outside of the LMNAmut cells by using the mechanoresponsive pathways of the actin cytoskeleton. However, presently, we cannot rule out the involvement of microtubules, as they are known to be connected to actin via kinesin 1 and to the nuclear membrane via nesprin-4.[3] Studies on nucleus and cytoskeletal elements co-transfected laminopathy cells could give insights on the precise mechanisms of nuclear rupture.

Substrate stiffness appears to modulate also nuclear integrity. Indeed, we detected that repetitive disruptions of the nuclear membrane, previously reported by De Vos et al.[16] in cells from different laminopathy patients under standard culturing conditions, are prevented on soft substrates (3 kPa) but increasingly occurs on stiffer substrates. It is not clear how the cells can survive a repetitive disruption of the nuclear membrane, as mixing of cytoplasmic and nuclear components prevents appropriate nuclear localization of nuclear factors that can be crucial for several mechanisms (such as replication, transcription).

Also PML-NBs, often lost from the nucleus in laminopathy cells cultured on a glass substrate, were retained in the nucleus of *LMNA*mut seeded on soft substrate. However, since we observed cytoplasmic localization of PML-NBs without nuclear abnormalities (**Fig. 6**), the presence of PML bodies in the cytoplasm is not indicative for disfunctions of the nuclear lamina. Moreover, in a parallel study a direct correlation between occurrence of cytoplasmic PML-NBs and nuclear rupture as seen with EYFP-NLS could not be established: while in some cases of nuclear rupture PML-NBs moved out of the nuclei, in other cases this did not happen. Conversely, leakage of PML-NB proteins into the cytoplasm or incomplete import of PML-NB proteins can cause cytoplasmic assembly of PML bodies without nuclear rupture.[16]

In conclusion, despite the fact that the data reported were from cells of only one laminopathy patient with rare compound mutation in the *LMNA* gene, our findings suggest that soft substrates could be used protect and possibly rescue cell from laminopathy patients with morphological disturbances and structural weakness. This study shows the value of using substrate stiffness based approach for improved diagnosis of genetically diseased cells in order to understand the interplay between genotype and phenotype. Elucidating the mechanotransduction

pathways involved in the response of *LMNA* mutated cells to changes in the extracellular environment will also help to provide new insight into the genotype phenotype correlations.

Materials and Methods

Cell cultures. Cells used in this study were primary skin fibroblasts. The laminopathies cells (*LMNA*mut) were obtained from a skin biopsy taken from a two-year-old male subject diagnosed with apparently typical Hutchinson Gilford progeria syndrome, which showed compound heterozygous mutations (*LMNA*^T528M/M540T).[18] Informed consent was obtained from the parents of the proband for this study. Normal human dermal fibroblasts (NHDFα) obtained from the European Collection of Cell Cultures (Salisbury, United Kingdom) were used as a control. Details about culturing can be found in **Supplemental Material**.

Transfection for live-cell imaging. *LMNA*mut were transiently transfected with an EYFP-NLS construct[33] (kind gift from Dr J. Goedhart, University of Amsterdam) using GeneJammer (Invitrogen, 204132) according to manufacturer's instructions at a GeneJammer/DNA ratio of 6:1 (microliter per microgram DNA). Transfection was performed 24 h after seeding of the cells and culture medium was changed 4 h after transfection to minimize cytotoxicity.

Coated polyacrylamide (PA) gels and glass substrates. Polyacrylamide (PA) gels coated with collagen I were used to create 2 dimensional substrates with controlled stiffness for NHDFα and *LMNA*mut. PA gel stiffness (expressed as elastic modulus, E) was controlled by modulating the bis-acrylamide crosslink concentration and was verified using an indentation test.[34] The method used for the preparation was adapted from Pelham and Wang.[35] Precursor mixtures of PA gels were made from acrylamide (40%, Sigma) and N, N′, N′-methylene-bisacrylamide (bis-AA, 2%, Sigma-Aldrich) mixed with MilliQ water and Hepes 50 mM. Final acrylamide concentrations were 5% or 10%, while bis-AA varied between 0.03% and 3%. Details of PA gels preparation can be found in **Supplemental Material**. Rat tail collagen I (BD biosciences) was covalently coupled the surfaces of the gels using the sulfo-SANPAH (Pierce Biotechnology) crosslinker in order to provide cellular attachment. The elastic modulus (E-modulus) of the PA gels was determined on gels prepared on coverslips (Menzel) with 25 µl of solution. Indentation was applied to the center of the gels with a spherical indenter (2 mm-diameter) while measuring force and indentation depth. Afterwards a numerical model was iteratively fitted to these experimental data using a parameter estimation algorithm. The mechanical properties of the PA gels were quantified in three gels for each group in the same day when the cells were seeded. The indentation test revealed that differences between the batches and in time were not significant (data not shown). The gels prepared with 5% acrylamide/0.01% bisacrylamide, 5% acrylamide/0.05% bisacrylamide 5% acrylamide/0.3% bisacrylamide, 10% acrylamide/0.26% bisacrylamide had elastic moduli of 3.8 ± 0.9, 9.9 ± 3.7, 19.8 ± 3.6 and 81.7 ± 2.4 kPa respectively (mean ± SD), as shown in **Table 1**. This stiffness range (3–80 kPa) was created to mimic physiologically-relevant stiffness values similar to fat tissue (3 kPa), muscle (10–20 kPa) and collagenous bone (> 20 kPa).

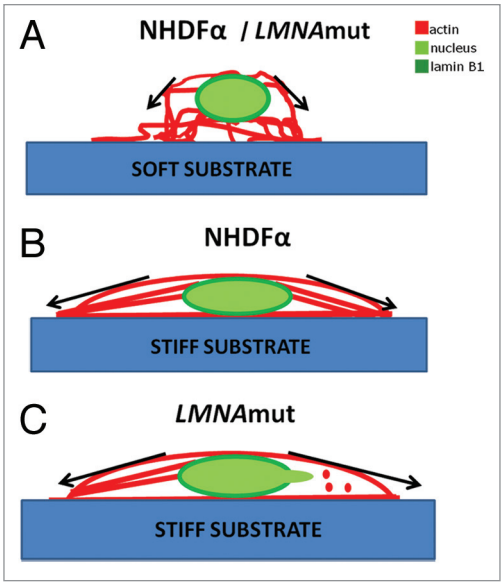

Figure 8. Proposed mechanism for actin cytoskeleton organization and effects on nuclear abnormalities on soft and stiff substrates. Schematic representation of the cross section of a cell seeded on substrates with different stiffness. Red represents the actin cytoskeleton while green the nucleus (dark green nuclear lamina). (**A**) When seeded on a soft substrate NHDFα and *LMNA*mut cells have the same response. They develop not tensed actin stress fibers which are not directly connected to the nucleus in the perinuclear region. Fibers run below and on top of the nucleus. Since low forces are exerted on the nucleus, the onset of nuclear abnormalities is prevented. (**B**) NHDFα cells seeded on a stiff substrate (stiffer than 3 kPa) develop tensed actin stress fibers which are well-organized in the whole cytoplasm. Stress fibers connect to the nucleus and form also the actin cap running on top of the nucleus. (**C**) *LMNA*mut cells on top of a stiff substrate develop tensed stress fibers. These stress fibers appear to be lacking in the perinuclear region and aggregates of actin are often visible. The pushing action of the actin cap (stress fibers running on top of the nucleus) together with the uneven distribution of pushing actin in the area around the nucleus lead to the development of nuclear abnormalities, further resulting in nuclear damage.

The glass substrates (coverslips No. 0, 13-mm diameter; Menzel), were sterilized in 70% ethanol and, subsequently, coated with adsorbed collagen I.

The covalent binding of collagen I coating to the substrates was examined by immunolabeling. The antibody used were mouse monoclonal antibody to collagen I (IGg1, diluted 1:100, Sigma-Aldrich) and, as secondary antibodies, goat anti-mouse IGg1 Alexa 488 (diluted 1:500, Molecular Probes).

Immunofluorescence labeling and imaging. At 48 h after seeding, NHDFα and *LMNA*mut grown onto PA gels of 3, 10, 20, 80 kPa and glass bottom culture dishes coated with collagen I were washed with PBS and fixed with 4% formaldehyde in PBS (Sigma-Aldrich) for 10 min at room temperature. Next, they were permeabilized with 0.1% Triton-X-100 (Merck) in PBS for 10 min and incubated with 2% bovine serum albumin

Table 1. Composition and elastic modulus of the polyacrylamide gels used as substrates

	3 kPa	10 kPa	20 kPa	80 kPa
Acrylamide	5%	5%	5%	10%
Bis-Acrylamide	0.01%	0.03%	0.3%	0.26%
E (kPa)	3.8 ± 0.9	9.9 ± 3.7	19.8 ± 3.6	81.7 ± 2

(BSA) in PBS in order to block non-specific binding. Afterwards, they were incubated for two hours with primary antibodies in NET-gel. The following primary antibodies were used: mouse MoAb to PML proteins (IgG1, diluted 1:200, sc-966, Santa Cruz) and rabbit polyclonal to lamin B1 (IgG1 1:500, diluted, ab16048, AbCam). After washing with PBS (three times, 10 min), secondary antibodies in NET-gel were applied for 1 h. Goat anti-mouse IgG1 Alexa 488 (diluted 1:500, Molecular Probes) was used against PML-NBs antibody while goat anti-rabbit IgG Alexa 555 or Alexa 488 (diluted 1:500, Molecular Probes) were used against lamin B1 antibody. For F-actin staining phalloidin-TRITC (1:200, Molecular Probes) was used. After two washing steps with PBS, cells were incubated for 5 min with DAPI (1:500, Molecular Probes) for nuclear counterstaining. Imaging for the immunofluorescence studies was performed by means of an inverted confocal microscope connected to an inverted Axiovert 200 M (Zeiss LSM 510 META, Zeiss). A C-Apochromat water-immersion objective (63 × NA = 1.2) was used to minimize the effects of spherical aberration when focusing deep into PA gels, while for cells plated on glass a Plan-Apochromat oil immersion objective was used (63 × , NA = 1.4). The laser scanning microscope was used in the dual parameter setup, according to the manufacturer's specification, using dual wavelength excitation: the Ar laser at 488 nm (30 mW) and the HeNe laser at 543 nm (1 mW). Z-series were generated by collecting a stack consisting of optical sections using a step size of 0.3–0.45 μm in the z-direction while a minimum pinhole opening was used (1AU). Alternatively, a Leica SPE confocal microscope was used, mounted on a DMI 4000 inverted microscope. Excitation lines were 405 nm (DAPI), 488 nm (FITC) and 532 nm (Phalloidin).

CytochalasinD treatment. At 24 h after seeding, *LMNA*mut grown onto collagen I coated glass bottom culture dishes were transiently treated with cytochalasin D (cytoD, Sigma-Aldrich) 1 μM to inhibit actin filament dynamics. Successively the growth medium was refreshed with normal growth medium. Three different treatments were performed:

• Short treatment + short recovery = 30 min cytoD treatment and 1 h recovery in normal growth medium

• Long treatment + short recovery = 3 h cytoD treatment and 1 h recovery in normal growth medium

• Long treatment + short recovery = 3 h cytoD treatment and overnight recovery in normal growth medium.

Finally, *LMNA*mut cells were fixed and stained for actin organization and nuclear abnormalities.

Cell spreading assay. Cells were detached using a trypsin solution containing 0.125% trypsin (Invitrogen Life Technologies, Breda, the Netherlands), 0.02 M EDTA and 0.02% glucose in PBS. Duration of trypsin treatment was kept to a minimum (approximately three min at 37°C), Trypsin was inactivated by adding an excess of culture medium with serum, and cells were seeded onto glass coverslips. Cells were allowed to attach for a variable period of time (0.5 h, 1 h, 2hr, 4 h, 8 h, 24 h or 72 h.) under standard culture conditions and were fixed and processed for immunofluorescence as described above. As primary antibody the mouse monoclonal lamin A/C antibody Jol2 (IgG1, diluted 1:20; a kind gift from Dr C.J. Hutchison (Durham University) was used. The percentage of cells with abnormal nuclei (blebs) was estimated by counting 3 × 100 cells per time point.

Image analysis. Brightfield images of cell cultures were obtained with an Axio Observer Z1 (Zeiss). For cell area and aspect ratio measurements, NHDFα and *LMNA*mut were manually outlined in relative brightfield images. Using ImageJ (1.45) freeware software, cell area and cell aspect ratio were measured. Cell aspect ratio was calculated as the length of the long axis of the cell divided by the length of the short axis. At least 60 cells were analyzed on the substrate of each type.

Abnormal nuclei or cytoplasmic PML bodies were scored manually on about 100 cells in three random locations on two samples per each stiffness (600 cells in total) for each cell genotype. Nuclei were scored as abnormally shaped when their appearance, after laminB1 staining and DAPI counterstaining, showed abnormalities such as blebs, large and poorly defined protrusions and invaginations. In scoring of PML bodies, a second non-specific channel was acquired (550LP) to avoid counting of autofluorescent foci. Mitotic cells, identified by the shape of the DAPI staining, were rejected from the analysis, as they also show cytoplamsic PML bodies.

Live cell imaging. In order to perform live cell-imaging, *LMNA*mut were seeded on PA gels of 3, 10, 20, 80 kPa and on glass bottom dishes and, after 24 h, were transfected with EYFP-NLS. After 24 to 36 h from transfection, *LMNA*mut were supplemented with pre-warmed phenol-free serum-containing culture medium (DMEM 31053, Invitrogen) complemented with 15 mM Hepes. Evaporation of the medium was prevented by covering it with an approximate 2 mm layer of mineral oil (Sigma) previously washed with culture medium. Time-lapse recording with an interval of one or two minutes were taken using an inverted automated microscope (Leica DMRBE) equipped with a black and white CCD-camera (CA4742–95). Image acquisition was achieved using Openlab software (Improvision). The microscope was equipped with a heated stage which temperature was set at 37°C. This allowed imaging the sample while keeping it in optimal cell culture conditions. A 20× (N.A.-0.45) objective was used. For image processing and analysis of time-lapse videos, ImageJ (1.45) freeware was used. Briefly, for each time-lapse recording the analysis of the fluctuations of the fluorescence intensity in representative nuclear regions was performed. Values were normalized and then plotted as function of the time.

Statistical analysis. Data are expressed as mean ± SEM and mean ± SD for PA gels elastic modulus. Statistical analysis was performed using StatGraphics (Manugistics, Inc.). The data were analyzed by unpaired t-test (allowing different SD), one-way ANOVA (followed by Tukey's multiple comparison test)

or, in case of non-Gaussian distribution, the Mann-Whitney or Kruskal Wallis tests (the latter when comparing more than two groups, followed by Tukey's multiple comparison test). A p-value of 0.05 was considered statistically significant.

Disclosure of Potential Conflicts of Interest

The authors declare that they have no financial interests in relation to the submitted work.

Acknowledgments

The authors are grateful to Cor Semeins, Emanuela Fioretta and Marloes Janssen-van den Broek for helping with protocol development, gel preparation and the many helpful discussions.

Supplemental Materials

Supplemental materials may be found here: www.landesbioscience.com/journals/nucleus/article/23388

References

1. Gilbert PM, Havenstrite KL, Magnusson KEG, Sacco A, Leonardi NA, Kraft P, et al. Substrate elasticity regulates skeletal muscle stem cell self-renewal in culture. Science 2010; 329:1078-81; PMID:20647425; http://dx.doi.org/10.1126/science.1191035.
2. Discher DE, Janmey P, Wang YL. Tissue cells feel and respond to the stiffness of their substrate. Science 2005; 310:1139-43; PMID:16293750; http://dx.doi.org/10.1126/science.1116995.
3. Wilson KL, Foisner R. Lamin-binding Proteins. Cold Spring Harb Perspect Biol 2010; 2:a000554; PMID:20452940; http://dx.doi.org/10.1101/cshperspect.a000554.
4. Crisp M, Liu Q, Roux K, Rattner JB, Shanahan C, Burke B, et al. Coupling of the nucleus and cytoplasm: role of the LINC complex. J Cell Biol 2006; 172:41-53; PMID:16380439; http://dx.doi.org/10.1083/jcb.200509124.
5. Huang H, Kamm RD, Lee RT. Cell mechanics and mechanotransduction: pathways, probes, and physiology. Am J Physiol Cell Physiol 2004; 287:C1-11; PMID:15189819; http://dx.doi.org/10.1152/ajpcell.00559.2003.
6. Broers JL, Machiels BM, Kuijpers HJ, Smedts F, van den Kieboom R, Raymond Y, et al. A- and B-type lamins are differentially expressed in normal human tissues. Histochem Cell Biol 1997; 107:505-17; PMID:9243284; http://dx.doi.org/10.1007/s004180050138.
7. Dahl KN, Ribeiro AJ, Lammerding J. Nuclear shape, mechanics, and mechanotransduction. Circ Res 2008; 102:1307-18; PMID:18535268; http://dx.doi.org/10.1161/CIRCRESAHA.108.173989.
8. Broers JL, Peeters EA, Kuijpers HJ, Endert J, Bouten CV, Oomens CW, et al. Decreased mechanical stiffness in LMNA-/- cells is caused by defective nucleocytoskeletal integrity: implications for the development of laminopathies. Hum Mol Genet 2004; 13:2567-80; PMID:15367494; http://dx.doi.org/10.1093/hmg/ddh295.
9. Lammerding J, Schulze PC, Takahashi T, Kozlov S, Sullivan T, Kamm RD, et al. Lamin A/C deficiency causes defective nuclear mechanics and mechanotransduction. J Clin Invest 2004; 113:370-8; PMID:14755334.
10. Vigouroux C, Auclair M, Dubosclard E, Pouchelet M, Capeau J, Courvalin JC, et al. Nuclear envelope disorganization in fibroblasts from lipodystrophic patients with heterozygous R482Q/W mutations in the lamin A/C gene. J Cell Sci 2001; 114:4459-68; PMID:11792811.
11. Muchir A, Medioni J, Laluc M, Massart C, Arimura T, van der Kooi AJ, et al. Nuclear envelope alterations in fibroblasts from patients with muscular dystrophy, cardiomyopathy, and partial lipodystrophy carrying lamin A/C gene mutations. Muscle Nerve 2004; 30:444-50; PMID:15372542; http://dx.doi.org/10.1002/mus.20122.
12. Sullivan T, Escalante-Alcalde D, Bhatt H, Anver M, Bhat N, Nagashima K, et al. Loss of A-type lamin expression compromises nuclear envelope integrity leading to muscular dystrophy. J Cell Biol 1999; 147:913-20; PMID:10579712; http://dx.doi.org/10.1083/jcb.147.5.913.
13. Nikolova V, Leimena C, McMahon AC, Tan JC, Chandar S, Jogia D, et al. Defects in nuclear structure and function promote dilated cardiomyopathy in lamin A/C-deficient mice. J Clin Invest 2004; 113:357-69; PMID:14755333.
14. De Vos WH, Houben F, Hoebe RA, Hennekam R, van Engelen B, Manders EM, et al. Increased plasticity of the nuclear envelope and hypermobility of telomeres due to the loss of A-type lamins. Biochim Biophys Acta 2010; 1800:448-58; PMID:20079404; http://dx.doi.org/10.1016/j.bbagen.2010.01.002.
15. Lee JS, Hale CM, Panorchan P, Khatau SB, George JP, Tseng Y, et al. Nuclear lamin A/C deficiency induces defects in cell mechanics, polarization, and migration. Biophys J 2007; 93:2542-52; PMID:17631533; http://dx.doi.org/10.1529/biophysj.106.102426.
16. De Vos WH, Houben F, Kamps M, Malhas A, Verheyen F, Cox J, et al. Repetitive disruptions of the nuclear envelope invoke temporary loss of cellular compartmentalization in laminopathies. Hum Mol Genet 2011; 20:4175-86; PMID:21831885; http://dx.doi.org/10.1093/hmg/ddr344.
17. Broers JL, Ramaekers FC, Bonne G, Yaou RB, Hutchison CJ. Nuclear lamins: laminopathies and their role in premature ageing. Physiol Rev 2006; 86:967-1008; PMID:16816143; http://dx.doi.org/10.1152/physrev.00047.2005.
18. Verstraeten VL, Broers JL, van Steensel MA, Zinn-Justin S, Ramaekers FC, Steijlen PM, et al. Compound heterozygosity for mutations in *LMNA* causes a progeria syndrome without prelamin A accumulation. Hum Mol Genet 2006; 15:2509-22; PMID:16825282; http://dx.doi.org/10.1093/hmg/ddl172.
19. Janmey PA, Euteneuer U, Traub P, Schliwa M. Viscoelastic properties of vimentin compared with other filamentous biopolymer networks. J Cell Biol 1991; 113:155-60; PMID:2007620; http://dx.doi.org/10.1083/jcb.113.1.155.
20. Malek AM, Izumo S. Mechanism of endothelial cell shape change and cytoskeletal remodeling in response to fluid shear stress. J Cell Sci 1996; 109:713-26; PMID:8718663.
21. Mizutani T, Haga H, Kawabata K. Cellular stiffness response to external deformation: tensional homeostasis in a single fibroblast. Cell Motil Cytoskeleton 2004; 59:242-8; PMID:15493061; http://dx.doi.org/10.1002/cm.20037.
22. Favreau C, Higuet D, Courvalin JC, Buendia B. Expression of a mutant lamin A that causes Emery-Dreifuss muscular dystrophy inhibits in vitro differentiation of C2C12 myoblasts. Mol Cell Biol 2004; 24:1481-92; PMID:14749366; http://dx.doi.org/10.1128/MCB.24.4.1481-1492.2004.
23. Khatau SB, Hale CM, Stewart-Hutchinson PJ, Patel MS, Stewart CL, Searson PC, et al. A perinuclear actin cap regulates nuclear shape. Proc Natl Acad Sci U S A 2009; 106:19017-22; PMID:19850871; http://dx.doi.org/10.1073/pnas.0908686106.
24. Houben F, Ramaekers FC, Snoeckx LH, Broers JL. Role of nuclear lamina-cytoskeleton interactions in the maintenance of cellular strength. Biochim Biophys Acta 2007; 1773:675-86; PMID:17050008; http://dx.doi.org/10.1016/j.bbamcr.2006.09.018.
25. Houben F, Willems CH, Declercq IL, Hochstenbach K, Kamps MA, Snoeckx LH, et al. Disturbed nuclear orientation and cellular migration in A-type lamin deficient cells. Biochim Biophys Acta 2009; 1793:312-24; PMID:19013199; http://dx.doi.org/10.1016/j.bbamcr.2008.10.003.
26. Borden KL. Pondering the promyelocytic leukemia protein (PML) puzzle: possible functions for PML nuclear bodies. Mol Cell Biol 2002; 22:5259-69; PMID:12101223; http://dx.doi.org/10.1128/MCB.22.15.5259-5269.2002.
27. Jul-Larsen AA, Grudic A, Bjerkvig R, Bøe SO. Cell-cycle regulation and dynamics of cytoplasmic compartments containing the promyelocytic leukemia protein and nucleoporins. J Cell Sci 2009; 122:1201-10; PMID:19339552; http://dx.doi.org/10.1242/jcs.040840.
28. Houben F, De Vos WH, Krapels IP, Coorens M, Kierkels GJ, Kamps MA, et al. Cytoplasmic localization of PML particles in laminopathies. Histochem Cell Biol 2013; 139:119-34; PMID:22918509; http://dx.doi.org/10.1007/s00418-012-1005-5.
29. Jensen BC. Skin deep: what can the study of dermal fibroblasts teach us about dilated cardiomyopathy? J Mol Cell Cardiol 2010; 48:576-8; PMID:20005233; http://dx.doi.org/10.1016/j.yjmcc.2009.11.021.
30. Capanni C, Cenni V, Mattioli E, Sabatelli P, Ognibene A, Columbaro M, et al. Failure of lamin A/C to functionally assemble in R482L mutated familial partial lipodystrophy fibroblasts: altered intermolecular interaction with emerin and implications for gene transcription. Exp Cell Res 2003; 291:122-34; PMID:14597414; http://dx.doi.org/10.1016/S0014-4827(03)00395-1.
31. Worman HJ, Fong LG, Muchir A, Young SG. Laminopathies and the long strange trip from basic cell biology to therapy. J Clin Invest 2009; 119:1825-36; PMID:19587457; http://dx.doi.org/10.1172/JCI37679.
32. Trappmann B, Gautrot JE, Connelly JT, Strange DG, Li Y, Oyen ML, et al. Extracellular-matrix tethering regulates stem-cell fate. Nat Mater 2012; 11:642-9; PMID:22635042; http://dx.doi.org/10.1038/nmat3339.
33. Kremers GJ, Goedhart J, van Munster EB, Gadella TW Jr. Cyan and yellow super fluorescent proteins with improved brightness, protein folding, and FRET Förster radius. Biochemistry 2006; 45:6570-80; PMID:16716067; http://dx.doi.org/10.1021/bi0516273.
34. Cox MA, Driessen NJ, Bouten CV, Baaijens FP. Mechanical characterization of anisotropic planar biological soft tissues using large indentation: a computational feasibility study. J Biomech Eng 2006; 128:428-36; PMID:16706592; http://dx.doi.org/10.1115/1.2187040.
35. Pelham RJ Jr., Wang Yl. Cell locomotion and focal adhesions are regulated by substrate flexibility. Proc Natl Acad Sci U S A 1997; 94:13661-5; PMID:9391082; http://dx.doi.org/10.1073/pnas.94.25.13661.